Pre-existing effector T-cell levels and augmented myeloid cell composition denote response to CDK4/6 inhibitor palbociclib and pembrolizumab in hormone receptor-positive metastatic breast cancer

Colt Egelston [iD] ,[1] Weihua Guo,[1] Susan Yost,[2] Jin Sun Lee,[2] David Rose,[1] Christian Avalos,[1] Jian Ye,[1] Paul Frankel,[3] Daniel Schmolze,[4] James Waisman,[2] Peter Lee,[1] Yuan Yuan[2]

Correspondence to
Yuan Yuan; yuyuan@coh.org

ABSTRACT

Background Single-agent pembrolizumab treatment of hormone receptor-positive metastatic breast cancer (MBC) has demonstrated modest clinical responses. Little is known about potential biomarkers or mechanisms of response to immune checkpoint inhibitors (ICIs) in patients with HR+ MBC. The present study presents novel immune correlates of clinical responses to combined treatment with CDK4/6i and ICI.

Methods A combined analysis of two independent phase I clinical trials treating patients with HR+ MBC was performed. Patients treated with the combination of the CDK4/6i palbociclib+the ICI pembrolizumab+the aromatase inhibitor (AI) letrozole (palbo+pembro+AI) were compared with patients treated with pembrolizumab+AI (pembro+AI). Peripheral blood mononuclear cells collected at pretreatment, 3 weeks (cycle 2 day 1) and 9 weeks (cycle 4 day 1) were characterized by high-parameter flow cytometry to assess baseline immune subset composition and longitudinal changes in response to therapy.

Results In the peripheral blood, higher pretreatment frequencies of effector memory CD45RA+ CD8+ T cells and effector memory CD4+ T cells were observed in responders to palbo+pembro+AI. In contrast, this was not observed in pembro+AI-treated patients. We further characterized T-cell subsets of effector-like killer cell lectin-like receptor subfamily G member 1 (KLRG1+) ICOS+ CD4+ T cells and KLRG1+ CD45RA+ CD8+ T cells as baseline biomarkers of response. In comparison, pretreatment levels of tumor-infiltrating lymphocyte, tumor mutation burden, tumor programmed death-ligand 1 expression, and overall immune composition did not associate with clinical responses. Over the course of treatment, significant shifts in myeloid cell composition and phenotype were observed in palbo+pembro+AI-treated patients, but not in those treated with pembro+AI. We identified increased fractions of type 1 conventional dendritic cells (cDC1s) within circulating dendritic cells and decreased classical monocytes (cMO) within circulating monocytes only in patients treated with palbociclib. We

also demonstrated that in palbociclib-treated patients, cDC1 and cMO displayed increased CD83 and human leukocyte antigen-DR isotype (HLA-DR) expression, respectively, suggesting increased maturation and antigen presentation capacity.

Conclusions Pre-existing circulating effector CD8+ and CD4+ T cells and dynamic modulation of circulating myeloid cell composition denote response to combined pembrolizumab and palbociclib therapy for patients with HR+ MBC.

Trial registration number NCT02778685 and NCI02648477.

INTRODUCTION

Immune checkpoint inhibitors (ICIs) targeting programmed cell death protein 1 (PD-1) or its ligand programmed death-ligand 1 (PD-L1) have emerged as effective therapeutic options for patients with triple-negative breast cancer (TNBC).[1] In the setting of metastatic TNBC, patients treated with the anti-PD-L1 antibody atezolizumab and nab-paclitaxel demonstrate increased progression-free survival benefit compared with those treated with nab-paclitaxel alone.[2] However, the role of ICIs in the treatment of hormone receptor-positive (HR+) breast cancer (BC) remains unclear. In preselected patients with PD-L1+HR+ metastatic breast cancer (MBC), single-agent pembrolizumab yielded a response rate (RR) of only 13%.[3] Evidence suggests that relative to TNBC, HR+ BC clinical outcome is less influenced by tumor-infiltrating lymphocyte (TIL) content, indicating immune surveillance mechanisms which may be specific to HR+ BC.[4] In the context of HR+ MBC, key immune mediators

dictating response to ICI-based treatments are largely not understood, and immune biomarkers predictive of response to these treatments are lacking. PD-L1 is a crucial protein for immune escape, and most clinical trials use PD-L1 as a predictive biomarker for response.[5] However, PD-L1 testing remains problematic across different clinical trials for ICI, and several studies have illustrated the imprecise nature of PD-L1 as a predictive biomarker. In a recent analysis, PD-L1 is predictive of response in only 28.9% of all ICI-treated patients.[6] Clearly, better pretreatment biomarkers of response to ICI are needed for patients with HR+ BC.

Clinical use of ICI in combination with targeted therapeutic agents is actively being investigated. The combination of a cyclin-dependent kinase 4 and 6 inhibitor (CDK4/6i) and an aromatase inhibitor (AI) or the selective estrogen receptor downregulator fulvestrant is the current standard-of-care therapy for patients with HR+ MBC.[7] CDK4/6i were primarily developed to curb increased cell proliferation associated with overactive CDK activity in cancer cells.[8] Recent preclinical evidence suggests that CDK4/6i may also modulate antitumor immune activity, including increased type III interferons, reduced regulatory T cells, and reduced suppressive myeloid cells.[9–11] Thus, clinical responses to CDK4/6i may result due to both cancer cell cytotoxicity and enhanced antitumor immunity. Therefore, a combinatorial strategy of CDK4/6i plus ICI may be an ideal therapeutic strategy for HR+ MBC. Preclinical exploration of combined CDK4/6i and ICI treatment in murine models of BC has shown efficacy and an increase in tumor microenvironment (TME) inflammation and T-cell activation.[12]

Two independent investigator-initiated phase I/II trials were conducted to study the safety and efficacy of the combination of palbociclib+the ICI pembrolizumab+the AI letrozole (palbo+pembro+AI) or pembro+AI in HR+ MBC. The current correlative study was conducted to identify potential biomarkers predicting response to the combination of CK4/6i and ICI in HR+ MBC. Here we characterize key features of patient immune composition in association with response to palbo+pembro+AI therapy. We identify circulating effector T-cell levels as a key requirement and predictive biomarker of response to the combination of CDK4/6i and ICI. Furthermore, by comparing palbo+pembro+AI-treated patients with pembro+AI treated patients, we demonstrate that modulation of circulating myeloid cells is a key feature of CDK4/6i. Together these data provide a clearer understanding of antitumor immune responses in patients with HR+ MBC treated with the combination of CDK4/6i and ICI.

METHODS

Sample collection

The clinical trial results have been presented and will be published in a separate manuscript.[13] Tumor specimen and peripheral blood were collected through two independent phase I trials: palbo+pembro+AI and pembro+AI. The primary objectives of the studies were to test the safety and tolerability of these therapies in HR+ MBC. Restaging CT scan and RECIST V.1.1 reading were performed every 12 weeks (one cycle=3 weeks). Tumor biopsies were collected prior to study initiation, and peripheral blood was collected at baseline (pretreatment), cycle 2 day 1 (C2D1), and cycle 4 day 1 (C4D1). Peripheral blood was obtained using heparin collection tubes, and peripheral blood mononuclear cells (PBMCs) were isolated within 6 hours using Ficoll-Paque separation according to manufacturer's instructions (GE Healthcare). PBMCs were cryopreserved in 10% dimethyl sulfoxide (DMSO), 90% fetal bovine serum (FBS) and thawed rapidly for flow cytometry analysis. Tumor biopsies were formalin-fixed paraffin-embedded.

Histological evaluation

Stromal tumor-infiltrating lymphocyte (sTIL) quantification of H&E-stained slides was performed according to the International Immuno-Oncology Biomarker Working Group on Breast Cancer Guidelines.[14] PD-L1 stain was performed using 22C3 antibody by Qualtek Molecular Laboratory.

Flow cytometry

Single-cell suspensions were prepared on ice in 2% FBS in phosphate-buffered saline (PBS). Antibody cocktails were diluted in Brilliant Violet Buffer (BD Biosciences). Samples were acquired using a BD Fortessa using FACS Diva V.6.1.3. Photomultiplier tube voltages were set using BD CS&T beads. Compensation was calculated using single-stained OneComp compensation beads (eBioscience). Samples were stained with fluorescently tagged antibodies detailed in online supplemental table 1. Antibodies were titrated for optimal signal to noise ratio prior to use. Flow cytometry analysis was performed using FlowJo V.X and the CATALYST R package was used for FlowSOM analysis and t-distributed stochastic neighbor embedding (tSNE) projections.[15] All samples were gated on live, single cells.

Tumor genomics analysis

Genomic analysis was performed with Tempus xT sequencing technology, including whole transcriptome RNA sequencing and a targeted 595 gene panel for assessment of nucleotide variants and tumor mutation burden (TMB).[16] STAR V.2.7 was used to align the sequences to the human genome. HT-seq was used to quantify the gene expression from aligned reads. The raw counts were normalized by edgeR. The batch effect was corrected by limma R package. CIBERSORTx was used to deconvolute the normalized and corrected RNA expression data to major immune cell types (LM22 signature) with 500 permutations for significance analysis.[17] Relative abundances of major immune cell types and the absolute score were compared between groups by Wilcoxon signed-rank test.

Statistics

Graphs and statistics were performed using GraphPad Prism V.8.4.3. Statistics were generated using unpaired two-tailed Student t-tests or multiple comparisons t-tests with Dunnet's or Holm-Sidak corrections as described. Calculated p values are displayed as *, p<0.05; **, p<0.01; ***, p<0.001; and ****, p<0.0001. For all graphs, the mean is represented by a line.

RESULTS

Higher frequencies of pre-existing circulating effector T cells predict response to palbociclib and pembrolizumab in HR+ MBC

HR+ MBC responders (complete response or partial response) and non-responders (stable disease or progressive disease) to palbo+pembro+AI treatment were identified per RECIST V.1.1. Patient tumor biopsies were assessed for common biomarkers of response to immunotherapy, including sTILs, tumor PD-L1 expression, and TMB. We found no significant differences in sTILs percentage (figure 1A), tumor PD-L1 expression (figure 1B), or TMB (figure 1C) between responders and non-responders to palbo+pembro+AI. We next sought to profile potential differences in tumor immune composition among our patients. CIBERSORT gene expression deconvolution analysis of tumor tissues was performed to assess both relative and absolute abundance of 18 different immune cell subsets (online supplemental figure 1). While tumors of responders demonstrated a trend in increased M0 macrophages and reduced M2 macrophages as compared with tumors of non-responders, no statistically significant differences were observed. Together, these data suggest a lack of significant differences in localized immune composition between HR+ MBC responders and non-responders to palbo+pembro+AI.

We next sought to identify baseline predictors of response by analyzing PBMCs from patients prior to treatment using two 15-parameter flow cytometry panels (gating strategy, online supplemental figures 1 and 2). Among the major lymphocyte populations, we found no differences in baseline frequencies of CD4+ T cells, CD8+ T cells, CD3+ CD56+ natural killer T cells, CD19+ B cells, or CD3− CD56+ natural killer cells (NKs) (figure 1D). We also observed no differences in frequencies of CD56^{bright}, CD16^{bright}, or CD56^{dim} CD16^{dim} NK subsets (figure 1E). Similarly, within myeloid populations, we found no differences in baseline frequencies of CD14+ CD16− classical monocytes (cMOs), CD14+CD16+ intermediate monocytes (iMOs), CD14− CD16+ non-classical monocytes (ncMOs), CD141+ type 1 conventional dendritic cells (cDC1s), CD1c+ type 2 conventional dendritic cells (cDC2s), or CD123+ plasmacytoid dendritic cells (pDCs) (figure 1F,G).

Specific T cell subsets have been correlated with response to ICI in other cancer settings.[18–20] We therefore next investigated traditional phenotypical and functional markers on T cells in our patient cohorts.
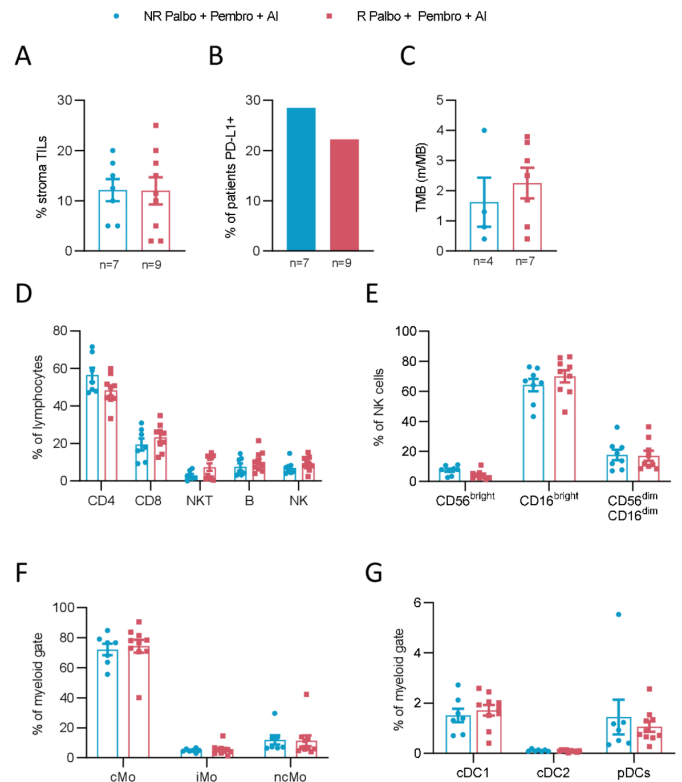

Figure 1 Baseline tumor and peripheral blood characterization of HR+ MBC responders and non-responders to palbo+pembro+AI. Baseline tumor biopsies were assessed for TILs (A), PD-L1 expression (B, reported as fraction of each cohort with PD-L1+ scored tumors), and tumor mutation burden (C, reported as m/MB). Baseline peripheral blood samples were examined by flow cytometry for lymphocyte composition frequencies, including CD4+ T cells, CD8+ T cells, CD3+ CD56+ NKTs, CD19+ B cells, or CD3− CD56+ NKs (D). The composition of NKs was further assessed for CD56^{bright}, CD16^{bright}, and CD56^{dim} CD16^{dim} NK subsets (E). Monocyte subsets were assessed as a fraction of a myeloid cell gate for frequencies of CD14+ CD16− cMOs, CD14+CD16+ iMOs, and CD14− CD16+ ncMOs (F). Dendritic cell subsets were similarly assessed as a fraction of a myeloid cell gate for frequencies of CD141+ dendritic cells (cDC1), CD1c+ dendritic cells (cDC2), and CD123+ pDCs (G). NR patients are depicted in blue; responder (R) patients are depicted in red. (D) NR, n=7; R, n=9. (E–G) NR, n=7; R, n=10. AI, aromatase inhibitor; cDC, conventional dendritic cell; cDC1, type 1 conventional dendritic cell; cDC2, type 2 conventional dendritic cell; cMO, classical monocyte; HR, hormone receptor; iMO, intermediate monocyte; m/MB, mutations/megabase; MBC, metastatic breast cancer; ncMO, non-classical monocyte; NK, natural killer; NKT, natural killer T cell; NR, non-responder; palbo, palbociclib; pDC, plasmacytoid dendritic cell; PD-L1, programmed death-ligand 1; pembro, pembrolizumab; R, responder; TIL, tumor-infiltrating lymphocyte; TMB, tumor mutation burden.

T-cell composition was assessed for frequencies of naïve (CCR7+ and CD45RA+), central memory (CM; CCR7+ and CD45RA−), effector memory (EM, CCR7− and CD45RA−), and effector memory CD45RA+ (EMRA, CCR7− and CD45RA+) subsets. Among CD8+ T cells, we observed reduced naïve cells and significantly higher frequencies
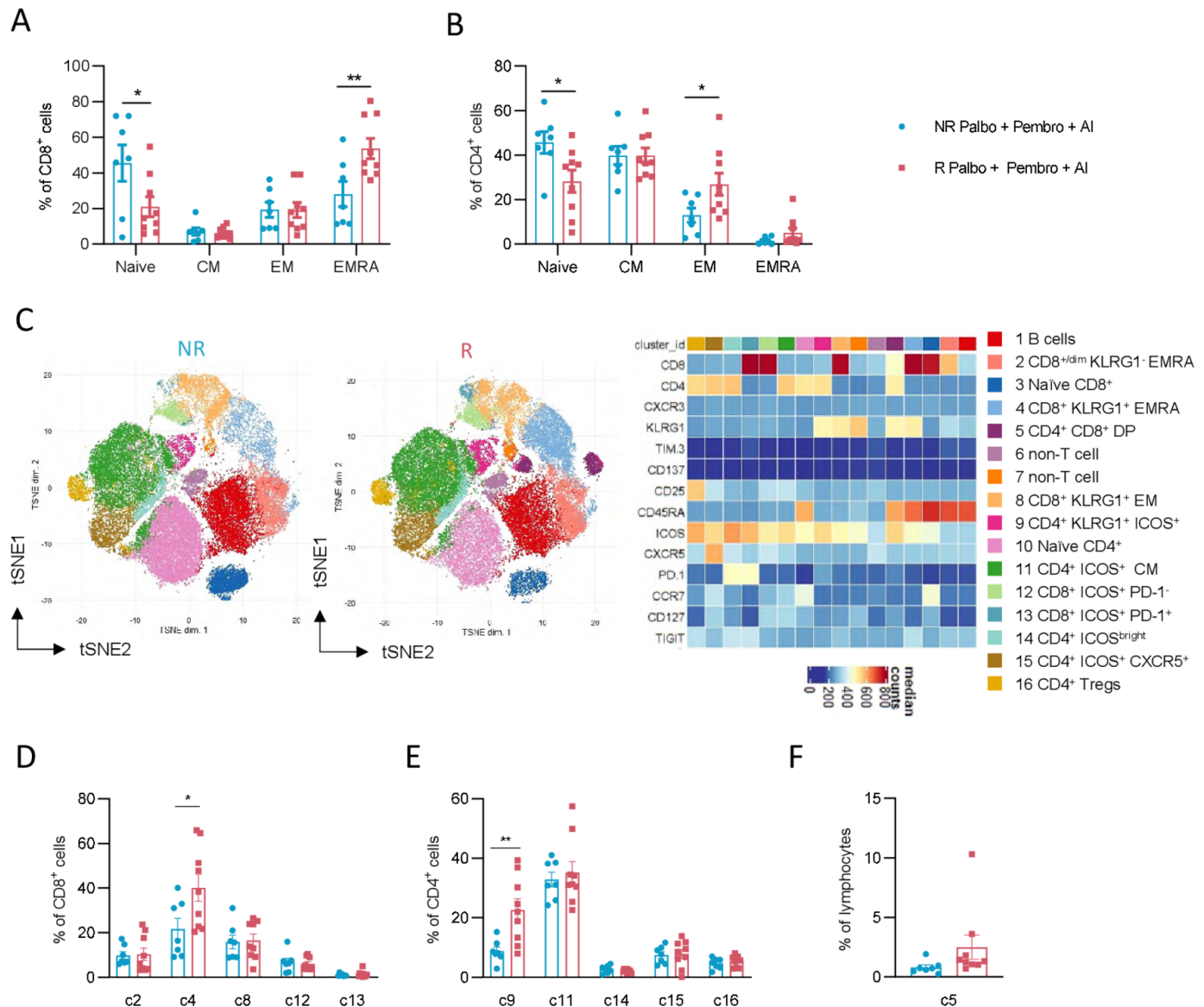
Figure 2 Distinct pre-existing effector T-cell subsets in responders to palbo+pembro+AI. CD8^{+} T cells (A) and CD4^{+} T cells (B) were further assessed by flow cytometry for naïve (CCR7^{+} and CD45RA^{+}), CM (CCR7^{+} and CD45RA^{−}), EM (CCR7^{−} and CD45RA^{−}), and EmrA (CCR7^{−} and CD45RA^{+}) cell subsets. Dimensionality reduction by the FlowSOM algorithm was performed to identify T-cell metaclusters in an unbiased manner as shown in t-distributed stochastic neighbor embedding (tSNE) projections of R and NR patients (C). A heatmap of identified clusters displays expression of various surface proteins used for each identified cell cluster. Percentages of identified non-naïve CD8^{+} T-cell clusters as a fraction of total CD8^{+} T cells are shown in NR and R patients (D). Percentages of identified non-naïve CD4^{+} T-cell clusters as a fraction of total CD4^{+} T cells are shown in NR and R patients (E). Percentages of non-classical CD4^{+} CD8^{+} DP cells and CD8^{dim} cells as a fraction of total lymphocytes (F). *P<0.05, **P<0.01; unpaired, two-tailed t-tests. NR patients are depicted in blue (n=7) and R patients are depicted in red (n=9). AI, aromatase inhibitor; CM, central memory; DP, double-positive; EM, effector memory; EMRA, effector memory CD45RA+; NR, non-responder; palbo, palbociclib; pembro, pembrolizumab; R, responder.

of EMRA cells in responder patients (figure 2A). Similar findings were seen among CD4^{+} T cells, with reduced naïve cells and increased EM cells in responder patients (figure 2B).

To further examine the pre-existing non-naïve T cells that were at higher levels in responder patients, we performed unbiased dimensionality reduction clustering analysis of our flow cytometry data using FlowSOM metacluster identification. Among lymphocytes assessed, 16 total clusters were identified, including two non-T/B-cell

clusters, one B-cell cluster, one CD4^{+} CD8^{+} cluster, six CD4^{+} T-cell clusters, and six CD8^{+} T-cell clusters (figure 2C). Since non-T-cell immune subset analyses were performed separately, we focused on five non-naïve CD8^{+} clusters, five non-naïve CD4^{+} clusters, and the CD4^{+} CD8^{+} double-positive population. Among CD8^{+} T-cell subsets, cluster c4, composed of killer cell lectin-like receptor subfamily G member 1 (KLRG1^{+}) CD45RA^{+} CD8^{+} T cells, was significantly higher in responder patients compared with non-responder patients (p value

of 0.01, responder 37.9% vs non-responder 14.8% of CD8$^+$ T cells (figure 2D). No differences between responder and non-responder patients were seen for frequencies of c2 (KLRG1$^-$ EMRA T cells), c8 (KLRG1$^+$ EM T cells), c12 (ICOS$^+$ PD-1$^-$ T cells), or c13 (ICOS$^+$ PD-1$^+$ T cells). Among CD4$^+$ T-cell subsets, we similarly found cluster c9 (KLRG1$^+$ ICOS$^+$ CD4$^+$ EM T cells) significantly higher in responder patients (p value of 0.007, responder 22.6% vs non-responder 8.7% of CD4$^+$ T cells) (figure 2E). No differences in frequencies of c11 (ICOS^{bright} T cells), c14 (ICOS$^+$ CCR7$^+$ CM T cells), c15 (ICOS$^+$ CXCR5$^+$ T cells), or c16 (CD25$^+$ CD127$^-$ Tregs) were observed between responder and non-responder patients. Finally, no differences in non-classical subsets c2 (CD8^{dim} T cells) or c5 (CD4$^+$ CD8$^+$ T cells) were found between responding and non-responding patients (figure 2F). Of note, both traditional gating strategies and our unbiased analysis approach found no significant differences in expression of the activation marker CD137 or checkpoint molecules TIM-3 or PD-1 between responder and non-responder patients. Instead, our data highlights the importance of pre-existing KLRG1$^+$ effector-like CD4$^+$ and CD8$^+$ T cells in enabling response to ICI in MBC.

Palbociclib treatment confers altered circulating myeloid cell composition and enables response to pembrolizumab

We next sought to dissect distinct immune surveillance alterations in patients over the course of treatment with palbo+pembro+AI compared with pembro+AI via flow cytometry. Our pembro+AI-treated patients yielded only 1 responder of 16 treated patients in line with published responses of 12% for patients with HR+ MBC.[3] We therefore focused research correlatives on comparing pembro+AI non-responders and palbo+pembro+AI responders. Compared with patient non-responders to pembro+AI, patient responders to palbo+pembro+AI demonstrated no differences at baseline in PBMC lymphocyte composition (figure 3A), CD8$^+$ T-cell composition (figure 3B), CD4$^+$ T-cell composition (figure 3C), NK subset composition (figure 3D), monocyte subset composition (figure 3E), or dendritic cell composition (figure 3F). The lack of immune composition differences, especially within T-cell subsets, between responder palbo+pembro+AI treated patients and non-responder pembro+AI-treated patients suggested that CDK4/6i played a role in enabling clinical responses to pembrolizumab.

To identify how palbociclib might mechanistically complement ICI, we next examined changes in immune composition relative to baseline in both trials. Pretreatment PBMCs were compared with precycle 2 treatment PBMCs by flow cytometry and examined for significant fold changes in population frequencies. Among all immune phenotypes assessed, myeloid cell compositional changes differed significantly between the two treatment cohorts (figure 3G). From baseline to C2D1, palbo+pembro+AI-treated patients demonstrated decreased cDC2s (CD141$^+$) (fold change 0.33 palbo+pembro+AI vs 1.2 pembro+AI, p value 0.001), decreased cMO

(fold change 0.71 palbo+pembro+AI vs 0.94 pembro+AI, p value 0.01), and increased pDCs (fold change 4.2 palbo+pembro+AI vs 0.89 pembro+AI, p value 0.06) as compared with pembro+AI-treated patients. Of note, pembro+AI-treated patients showed a greater decrease in naïve CD8$^+$ T cells (c3; fold change 1.08 palbo+pembro+AI vs 0.76 pembro+AI, p value 0.004) as compared with palbo+pembro+AI-treated patients. No other significant differences in lymphocyte population fold changes were found between the two treatment cohorts. Thus, changes in circulating myeloid cell composition, especially large decreases in the numbers of cDC2 and cMO and a modest increase (although not statistically significant) in the numbers of pDCs were identified in patients treated with palbociclib.

We next examined changes in myeloid cell composition from both pretreatment to cycle 2 and pretreatment to cycle 4 in palbo+pembro+AI compared with pretreatment to cycle 2 pembro+AI-treated patients. Within total myeloid cells, cDC1 frequencies were not observed to be significantly differentially perturbed in palbo+pembro+AI-treated patients compared with pembro+AI-treated patients (figure 4A). However, cDC2s were decreased significantly by both cycle 2 and cycle 4 in palbo+pembro+AI-treated patients (figure 4B). This decrease was not observed in cycle 2 pembro+AI-treated patients (p value 0.005, mean decrease −0.06% change in palbo+pembro+AI cycle 2 compared with mean increase 0.01% in pembro+AI cycle 2). In several patients, circulating cDC2s were not observed at cycle 2 and cycle 4 timepoints, highlighting that cDC2s are a small fraction of circulating myeloid cells highly sensitive to palbociclib treatment. pDCs, a larger population within circulating myeloid cells, trended towards an increased frequency of circulating myeloid cells over the course of palbo+pembro+AI treatment (figure 4C). However, this increase in frequency did not reach statistical significance compared with the pembro+AI cohort (p value 0.07, 3.4% mean increase in palbo+pembro+AI cycle 2 compared with −0.05% decrease in pembro+AI cycle 2). Finally, we found that cMO frequencies decreased significantly over the course of treatment in the palbo+pembro+AI cohort but not in the pembro+AI cohort (figure 4D). As cMO constituted a large fraction of circulating myeloid cells, the changes in frequencies observed were large (p value 0.01, mean decrease −19.3% palbo+pembro+AI cycle 2 compared with −1.29% pembro+AI cycle 2). Likely as a result of the decrease in cMO, iMO (figure 3E) and ncMO (figure 3F), frequencies of circulating myeloid cells trended towards increasing over the course of palbo+pembro+AI treatment, but changes were not significantly different compared with pembro+AI-treated patients.

Hematological toxicity, especially neutropenia, is a known side effect of CDK4/6i.[7] We therefore assessed if changes in monocyte composition and clinical responses in palbo+pembro+AI-treated patients simply reflected depletion of circulating white blood cells (WBCs). As
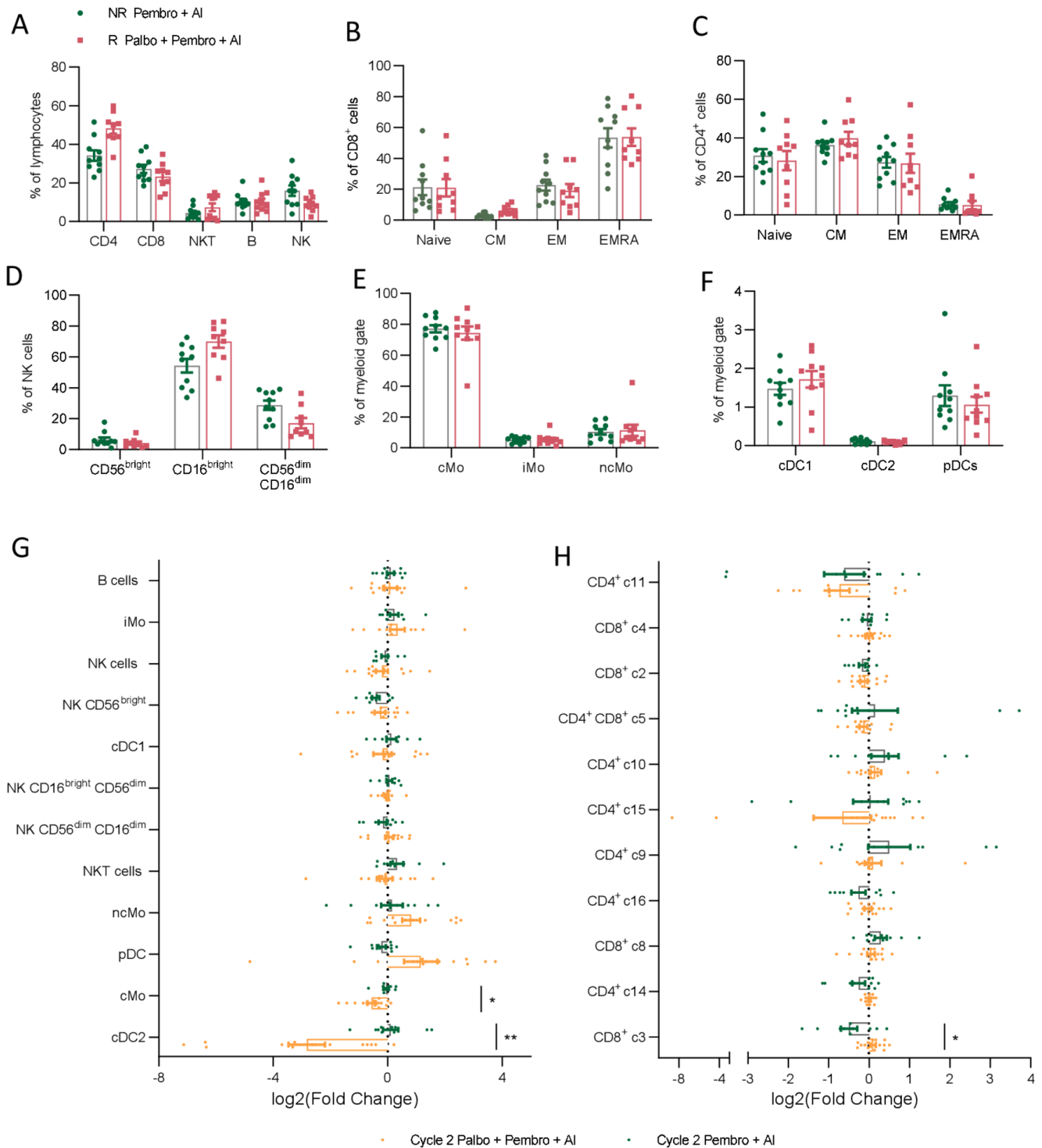
Figure 3 Peripheral immune composition changes in Rs to palbo+pembro+AI compared with NRs to pembro+AI. Baseline immune subset composition in responders to palbo+pembro+AI treatment (red) was compared with non-responders to pembro+AI treatment (green). Major lymphocyte subsets (A), CD8+ T-cell memory subsets (B), CD4+ T-cell memory subsets (C), NK subsets (D), monocyte subsets (E), and dendritic cell subsets (F) were assessed by flow cytometry. Changes in immune composition from baseline to C2D1 were also assessed by flow cytometry for all major non-T-cell immune subsets (G) and T-cell clusters previously identified (H) by calculating fold change from baseline. Log2 transformed fold changes are depicted and populations are sorted from least significant difference (top) to most significant difference (bottom). C2D1 palbo+pembro+AI (gold); C2D1 pembro+AI (green). *P<0.05, **P<0.01; unpaired, two-tailed t-tests. (A–C) R: palbo+pembro+AI, n=9; NR: pembro+AI, n=10. (DcF) R: palbo+pembro+AI, n=10; NR: pembro AI, n=10. (G–H) palbo+pembro+AI, n=14; pembro+AI, n=10. AI, aromatase inhibitor; C2D1, cycle 2 day 1; cDC1, type 1 conventional dendritic cell; cDC2, type 2 conventional dendritic cell; CM, central memory; cMO, classical monocyte; EM, effector memory; EMRA, effector memory CD45RA+; iMO, intermediate monocyte; ncMO, non-classical monocyte; NK, natural killer cell; NKT, natural killer T cell; NR, non-responder; palbo, palbociclib; pDC, plasmacytoid dendritic cell; pembro, pembrolizumab; R, responder.
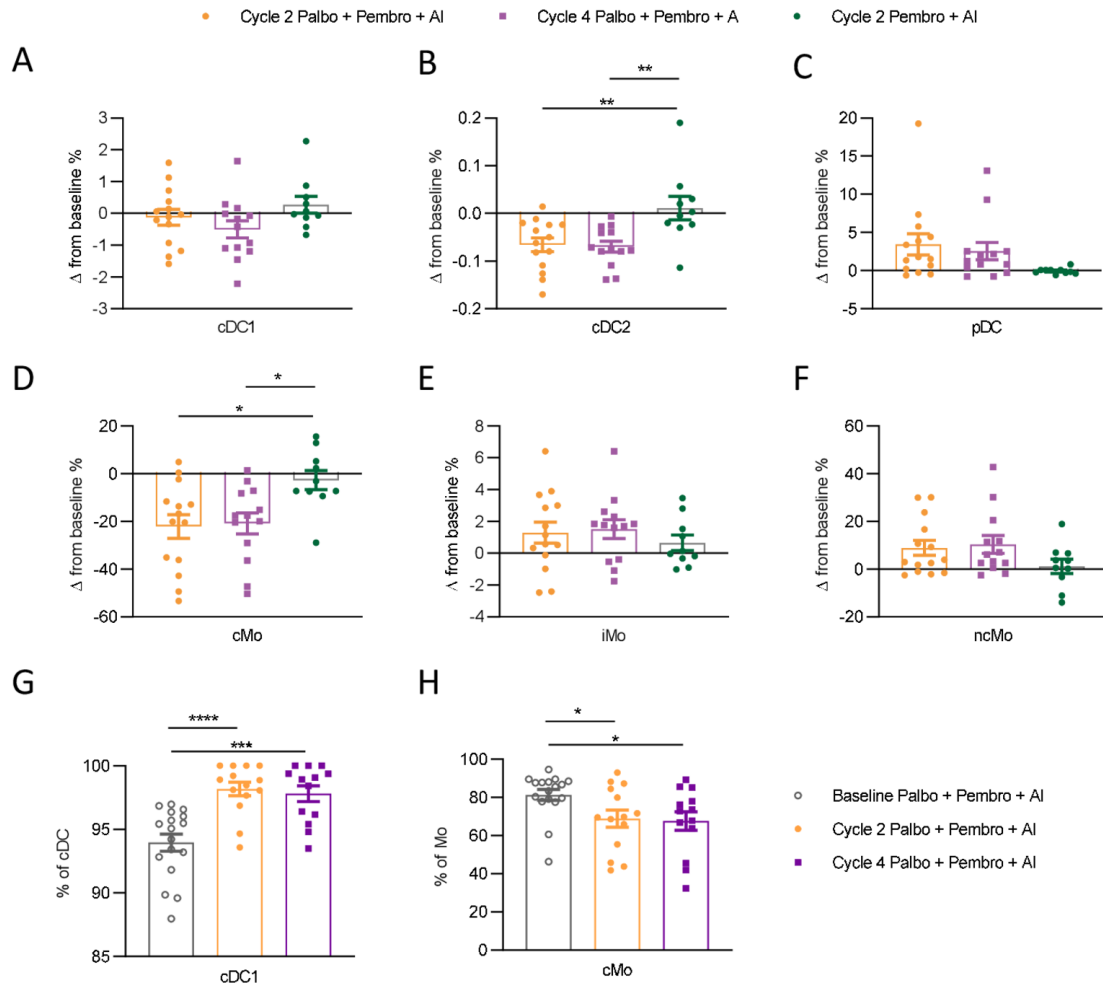
Figure 4 Dynamic peripheral myeloid cell changes in patients treated with palbo+pembro+AI compared with pembro+AI Changes in cell population percentages over the course of therapy were compared between palbo+pembro+AI-treated and pembro+AI-treated patients. Changes in frequencies of cDC1 (A), cDC2 (B), pDC (C), cMO (D), iMO (E), and ncMO (F) were evaluated as fractions of myeloid cell gates. (A–F) Data are normalized by subtraction of cell population percentages identified at baseline in the same patient. cDC1 frequencies among total circulating dendritic cells (cDC1+cDC2) are shown over the course of treatment (G). cMO frequencies among total circulating monocytes (cMO+iMO+ncMO) are shown over the course of treatment (H). Baseline palbo+pembro+AI depicted by gray open circle (n=17); C2D1 palbo pembro+AI depicted in gold (n=14); C4D1 palbo+pembro+AI depicted in purple (n=13), C2D1 pembro+AI depicted in green (n=10). *P<0.05, **P<0.01, ***P<0.001, ****P<0.0001; Dunnett's multiple comparisons test. AI, aromatase inhibitor; C2D1, cycle 2 day 1; C4D1, cycle 4 day 1; cDC1, type 1 conventional dendritic cell; cDC2, type 2 conventional dendritic cell; cMO, classical monocyte; iMO, intermediate monocyte; ncMO, non-classical monocyte; palbo, palbociclib; pDC, plasmacytoid dendritic cell; pembro, pembrolizumab.

expected, complete blood counts (CBCs) showed significant reduction of WBCs from pretreatment to cycle 2 (online supplemental figure 4A). cMO frequencies but not iMO or ncMO were significantly reduced from baseline to cycle 2 (online supplemental figure 4B). Importantly, CBCs of monocytes, lymphocytes, and neutrophils were all reduced similarly in responder and non-responder patients (online supplemental figure AC–E). Thus, while palbociclib treatment results in a marked decrease in circulating WBC counts, our flow cytometry data suggest that palbociclib may alter circulating myeloid cell composition by preferentially reducing the fraction of total monocytes made up of cMO and increasing the fraction of cDC made up of cDC (figure 4G,H). Furthermore, we did not find any statistical differences between responder and non-responder patients in changes in

myeloid cell frequencies over the course of palbo+pembro+AI treatment (online supplemental figure 5). These findings enforced that both myeloid cell modulation and the presence of pre-existing effector T cells are necessary for clinical responses in patients with HR+ BC.

Palbociclib treatment results in increased frequencies of mature cMOs and mature cDC1 dendritic cells

Given that we observed compositional changes in circulating myeloid cells over the course of palbociclib treatment, we next asked if palbociclib might alter the maturation state of myeloid cell subsets. Increased CD83 expression, a marker of increased DC maturation, was observed on cDC1 cells over the course of treatment with palbo+pembro+AI (figure 5A). This effect was not observed in pembro+AI-treated patients (p value 0.0001,
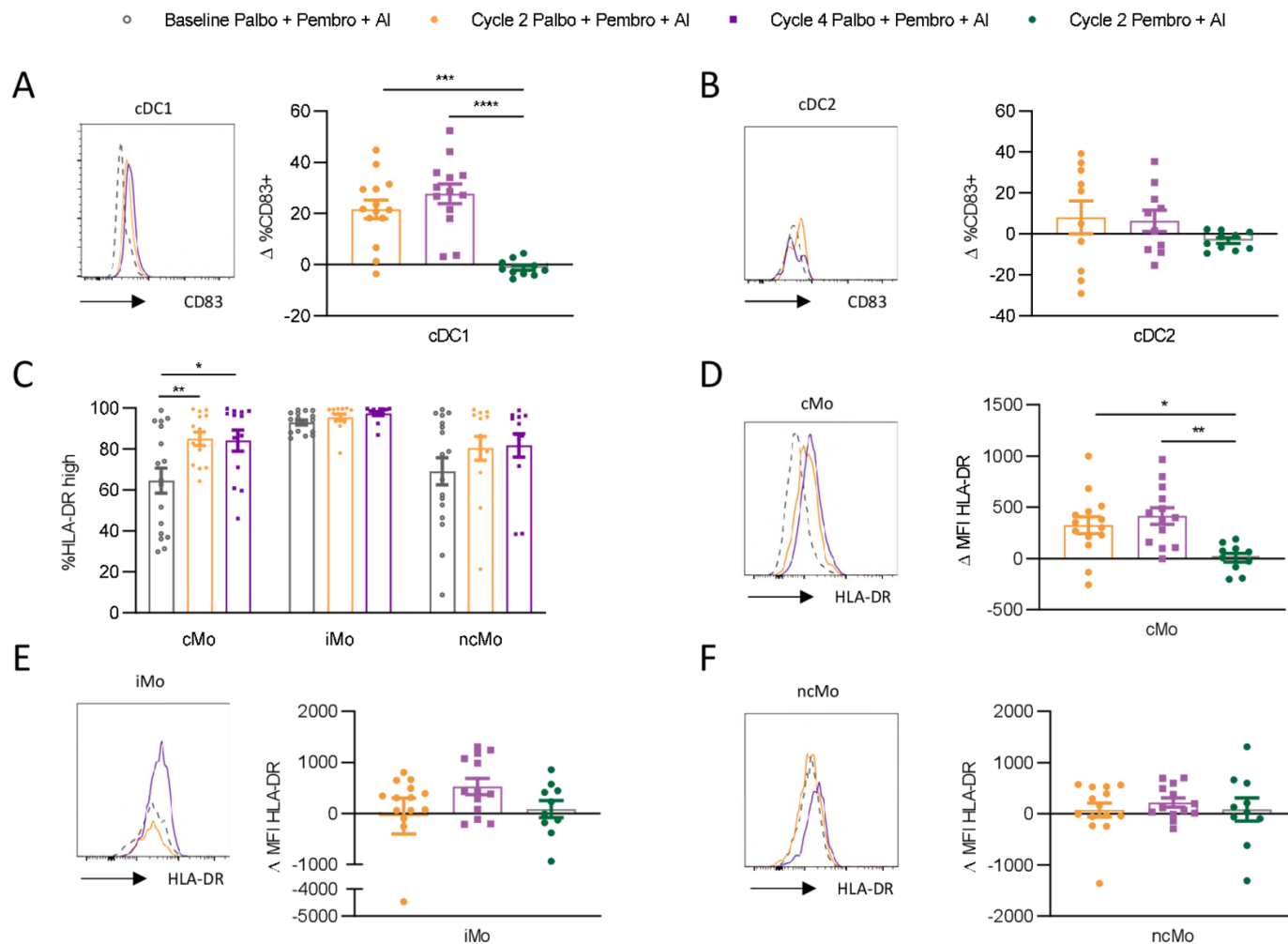
Figure 5 Palbociclib yields increased frequencies of circulating mature cDC1 and cMOs. Circulating dendritic cell and monocyte subsets were assessed by flow cytometry for changes in maturation status over the course of therapy. Changes in CD83 expression compared with baseline pretreatment were examined in cDC1 (A) and cDC2 (B) cells. Monocyte subsets were examined for changes in frequencies of human leukocyte antigen-DR isotype (HLA-DR)high cells compared with baseline (C). Changes in HLA-DR expression as measured by change in MFI relative to baseline MFI on the same cell subsets was assessed in cMO (D), iMO (E), and ncMO (F). Representative histograms are shown, with the dotted line displaying matched baseline cell subset marker expression. Baseline palbo+pembro+AI depicted by gray open circle (n=17); C2D1 palbo+pembro+AI depicted in gold (n=14); C4D1 palbo+pembro+AI depicted in purple (n=13), C2D1pembro+AI depicted in green (n=10). *P<0.05, **P<0.01, ***P<0.001, ****P<0.0001; Dunnett's multiple comparisons test. AI, aromatase inhibitor; C2D1; cycle 2 day 1; C4D1, cycle 4 day 1; cDC1, type 1 conventional dendritic cell; cDC2, type 2 conventional dendritic cell; cMO, classical monocyte; iMO, intermediate monocyte; MFI, median fluorescent intensity; ncMO, non-classical monocyte; palbo, palbociclib; pDC, plasmacytoid dendritic cell; pembro, pembrolizumab.

mean increase palbo+pembro+AI cycle 2 compared with mean decrease pembro+AI cycle 2 was 21.5% and −1.2%, respectively). CD83 expression by cDC2 was not found to be significantly affected by treatment, although we note that our ability to assess this was limited by the large reduction in cDC2 cell numbers (figure 5B).

In monocytes, higher human leukocyte antigen-DR isotype (HLA-DR) expression is associated with increased maturation and T-cell priming capacity, while lower HLA-DR expression is associated with immunosuppressive features.[21] Similarly, we found HLA-DR expression to be highest on iMO, with mixed expression levels on cMO and ncMO (figure 5C). Over the course of palbo+pembro+AI treatment, HLA-DRhigh expressing cells significantly increased

only among cMO (p value 0.005 baseline to cycle 2, mean difference 20.5%; p-value 0.01 baseline to cycle 4, mean difference 19.6%). Increased HLA-DR expression was not found in pembro+AI-treated patients (figure 5D) and was significantly greater in palbo+pembro+AI-treated patients (p value 0.01; mean increased HLA-DR MFI in palbo+pembro+AI cycle 2 compared with mean increase in pembro+AI cycle 2 was 415 and 8.9, respectively). Significant changes in HLA-DR expression by iMO and ncMO were not observed over the course of treatment (figure 5E,F).

DISCUSSION

Our study was performed to understand the composition and dynamics of host immune responses and tumor

immune composition in patients with HR+ MBC undergoing combination therapy of CDK4/6i palbociclib and ICI pembrolizumab. Key pre-existing and modulated immune subsets that define patients with clinical responses to therapy were identified. Higher baseline frequencies of effector T cells were observed in patients responding to combination CDK4/6i and anti-PD-1 therapy (palbo+pembro+AI cohort). However, non-responder patients treated with anti-PD-1 therapy with no CDK4/6i (pembro+AI cohort) showed no differences in baseline effector T-cell levels. This suggests that a pre-existing host circulating T-cell response is necessary but not sufficient for clinical response to ICI in HR +MCB.

Palbociclib modulation of circulating myeloid cells may explain the increased RR in palbo+pembro+AI-treated patients compared with pembro+AI-treated patients. Palbo+pembro+AI-treated patients demonstrated significantly reduced cDC2 numbers in peripheral blood, resulting in an increased fraction of cDC1 making up the circulating cDC population. On-treatment cDC1 cells displayed increased CD83 expression, suggesting increased maturation. Similarly, palbo+pembro+AI-treated patients had reduced fractions of cMO among circulating monocytes. Remaining on-treatment cMO displayed increased expression of HLA-DR, resulting in reduced fractions of HLA-DR^{low} cMO. Thus, our findings demonstrate that concurrently enabling a pre-existing T-cell response and promoting favorable myeloid cell compositions are key features of therapeutic response to CDK4/6i and ICI in patients with HR+ MBC.

The presence and density of TILs, PD-L1 expression, and TMB are established biomarkers of response to ICI-based therapies in many solid tumor settings.[22] Notably, pretreatment tumor TILs, PD-L1 expression, and TMB, consistent with historical data of immune cold HR +BC, were not associated with responses to palbo+pembro+AI therapy. Instead, we found peripheral immune biomarkers, both at baseline and over the course of therapy, that correlate with therapeutic response. Evidence connecting various pre-existing circulating T-cell populations with response to ICI has been found in patients with non-small cell lung cancer (NSCLC) and melanoma. Higher fractions of both CD4$^+$ and CD8$^+$ central memory T cells correlated with response to nivolumab in patients with NSCLC.[23] In patients with melanoma, higher fractions of circulating memory CD8$^+$ T cells correlated with response to ipilimumab and increased survival.[24] Our results in HR+ MBC identify elevated frequencies of pre-existing KLRG1$^+$ EMRA CD8$^+$ T cells and KLRG1$^+$ ICOS$^+$ EM CD4$^+$ T cells as important subsets that are predictive of response to ICI in HR+ MBC. EMRA CD8$^+$ T cells have also been shown to be important biomarkers of response to ICI in nivolumab-treated patients with NSCLC.[25] Whether EMRA CD8$^+$ T cells are mediators of tumor rejection themselves or are simply reflective of a systemic T-cell response is unclear. EMRA CD8$^+$ T cells are generally considered differentiated T cells found predominantly in the circulation from which they potentially traffic into peripheral tissues.[26]

KLRG1 is generally considered a marker of effector T cells upregulated after proliferation.[27] Thus, KLRG1 expression by EMRA CD8$^+$ T cells may indicate recent activation in peripheral lymph nodes, and recent data have suggested that these cells may have the capacity to generate memory T cells.[28] As such, circulating KLRG1+ T cells may be a significant cellular target of anti-PD-1 ICI therapies.

Dynamic changes in immune subset composition have been observed in patients treated with ICI. Ipilimumab has been shown to increase circulating CD4$^+$ ICOS$^+$ effector T cells in patients with bladder and melanoma cancers.[29–31] Anti-PD-1-based ICI therapies may preferentially induce expansion of CD8$^+$ T-cell subsets.[18 19] Specifically, proliferative CD8$^+$ effector T cells have been shown to increase in the circulation of patients with NSCLC receiving anti-PD-1 blocking antibodies and are associated with a positive outcome.[32] Furthermore, proliferative CD8$^+$ T cells have been observed to peak in peripheral blood of patients with melanoma within 7 days of the first dose of pembrolizumab.[33] In this small study, we did not observe significant expansion or activation of T-cell subsets over the course of treatment with pembrolizumab. Instead, our results highlight the importance of a pre-existing CD8$^+$ and CD4$^+$ T-cell response for response to ICI therapy in HR+ MBC. Further studies characterizing circulating effector T-cell subsets and dynamic changes of TME that denote response to palbo+pembro+AI are currently being carried out in larger patient cohorts.

Shifting myeloid cell composition towards one composed of cell subsets with more antitumor phenotypes is increasingly being recognized as a requirement for antitumor T-cell activity.[34 35] Circulating HLA-DR^{low} monocytes have been associated with increased disease progression in patients with MBC.[36] Our findings show that palbociclib treatment reduces the presence of HLA-DR^{low} cMO, which is in agreement with findings in preclinical models of BC.[37] cMOs are thought to be the primary source of tumor-associated macrophages (TAMs) which tend to exhibit protumorigenic features.[38–40] Preclinical evidence suggests that circulating monocytes may infiltrate metastatic tissues and differentiate into immunosuppressive macrophages.[41] Thus, increased fractions of circulating HLA-DR^{high} cMO mediated by palbociclib may result in tumor infiltration of macrophages with increased antigen presentation capacity. Further work to elucidate tumor localized effects of palbociclib therapy on TAM composition is ongoing.

Tumor infiltrating cDC1 dendritic cells have previously been shown to be critical for trafficking of peripheral effector T cells into tumor tissues.[42] Additionally, cDC1s are necessary for response to anti-PD-1 therapy in murine cancer models.[43] Recently, PD-L1+ dendritic cells have been identified to be important in regulating antitumor T-cell immunity and are potentially a key target for anti-PD-1/PD-L1 therapy.[44] We show that palbociclib treatment not only increases the fraction of circulating cDC1 dendritic cells but also yields increased fractions of

mature CD83^{+} cDC1 cells. Thus, treatment with palbociclib may enhance cDC1 boosting of the pre-existing antitumor T-cell response that is further accelerated in combination with pembrolizumab treatment. While we find that palbociclib treatment promotes increased frequencies of both CD83^{+} cDC1 and HLA-DR^{high} cMO, it is still unclear how this translates to enhanced TME localized antitumor immunity. Further work is needed to elucidate how CDK4/6i alters myeloid composition in the TME and affects interactions between antigen-presenting cells and T cells.

Biomarkers, either baseline or dynamic, that can predict response to ICI are urgently needed to inform future clinical trials for HR+ MBC. In this small cohort, we find strong evidence for the necessity of pre-existing effector T cells for response to CDK4/6i and ICI in patients with HR+ MBC. Although pre-existing peripheral effector T cells are necessary, they are not sufficient for clinical responses without additional intervention. Our study adds to previous preclinical studies providing evidence that CDK4/6i enhances antitumor immunity. The convergent mechanisms of palbociclib CDK4/6 inhibiting cell-cycle and myeloid population compositional changes may enable response to ICI in HR+ MBC. Further work is needed to explore mechanisms of palbociclib and pembrolizumab combinatorial therapy, especially to correlate immune changes in peripheral blood with tumor localized cancer cell cytotoxicity.

Author affiliations
[1]Immuno-oncology, Beckman Research Institute City of Hope, Duarte, California, USA
[2]Medical Oncology, City of Hope National Medical Center, Duarte, California, USA
[3]Biostatistics, Beckman Research Institute City of Hope, Duarte, California, USA
[4]Pathology, City of Hope National Medical Center, Duarte, California, USA

Twitter Colt Egelston @ColtEgelston

ORCID iD
Colt Egelston http://orcid.org/0000-0001-8440-1271

REFERENCES

1. Narayan P, Wahby S, Gao JJ, et al. Fda approval summary: Atezolizumab plus paclitaxel protein-bound for the treatment of patients with advanced or metastatic TNBC whose tumors express PD-L1. *Clin Cancer Res* 2020;26:2284–9.
2. Schmid P, Adams S, Rugo HS, et al. Atezolizumab and nab-paclitaxel in advanced triple-negative breast cancer. *N Engl J Med* 2018;379:2108–21.
3. Rugo HS, Delord J-P, Im S-A, et al. Safety and antitumor activity of pembrolizumab in patients with estrogen Receptor-Positive/Human epidermal growth factor receptor 2-Negative advanced breast cancer. *Clin Cancer Res* 2018;24:2804–11.
4. Loi S, Sirtaine N, Piette F, et al. Prognostic and predictive value of tumor-infiltrating lymphocytes in a phase III randomized adjuvant breast cancer trial in node-positive breast cancer comparing the addition of docetaxel to doxorubicin with doxorubicin-based chemotherapy: big 02-98. *J Clin Oncol* 2013;31:860–7.
5. Patel SP, Kurzrock R. Pd-L1 expression as a predictive biomarker in cancer immunotherapy. *Mol Cancer Ther* 2015;14:847–56.
6. Davis AA, Patel VG. The role of PD-L1 expression as a predictive biomarker: an analysis of all US food and drug administration (FDA) approvals of immune checkpoint inhibitors. *J Immunother Cancer* 2019;7:278.
7. Spring LM, Wander SA, Zangardi M, et al. CDK 4/6 inhibitors in breast cancer: current controversies and future directions. *Curr Oncol Rep* 2019;21:25.
8. Finn RS, Martin M, Rugo HS, et al. Palbociclib and letrozole in advanced breast cancer. *N Engl J Med* 2016;375:1925–36.
9. Deng J, Wang ES, Jenkins RW, et al. CDK4/6 inhibition augments antitumor immunity by enhancing T-cell activation. *Cancer Discov* 2018;8:216–33.
10. Teo ZL, Versaci S, Dushyanthen S, et al. Combined CDK4/6 and PI3Kα inhibition is synergistic and immunogenic in triple-negative breast cancer. *Cancer Res* 2017;77:6340–52.
11. Goel S, DeCristo MJ, Watt AC, et al. CDK4/6 inhibition triggers anti-tumour immunity. *Nature* 2017;548:471–5.
12. Schaer DA, Beckmann RP, Dempsey JA, et al. The CDK4/6 inhibitor Abemaciclib induces a T cell inflamed tumor microenvironment and enhances the efficacy of PD-L1 checkpoint blockade. *Cell Rep* 2018;22:2978–94.
13. Yuan Y, Yost SE, Lee JS. Abstract P3-11-04: a phase II study of pembrolizumab, letrozole and palbociclib in patients with metastatic estrogen receptor positive breast cancer. *Cancer Research* 2020.

14 Salgado R, Denkert C, Demaria S, *et al*. The evaluation of tumor-infiltrating lymphocytes (TILs) in breast cancer: recommendations by an international TILs Working group 2014. *Ann Oncol* 2015;26:259–71.

15 Chevrier S, Crowell HL, Zanotelli VRT, *et al*. Compensation of signal spillover in suspension and imaging mass cytometry. *Cell Syst* 2018;6:612–20.

16 Beaubier N, Tell R, Lau D, *et al*. Clinical validation of the tempus xT next-generation targeted oncology sequencing assay. *Oncotarget* 2019;10:2384–96.

17 Newman AM, Liu CL, Green MR, *et al*. Robust enumeration of cell subsets from tissue expression profiles. *Nat Methods* 2015;12:453–7.

18 Sade-Feldman M, Yizhak K, Bjorgaard SL, *et al*. Defining T cell states associated with response to checkpoint immunotherapy in melanoma. *Cell* 2018;175:998–1013.

19 Im SJ, Hashimoto M, Gerner MY, *et al*. Defining CD8+ T cells that provide the proliferative burst after PD-1 therapy. *Nature* 2016;537:417–21.

20 Thommen DS, Koelzer VH, Herzig P, *et al*. A transcriptionally and functionally distinct PD-1+ CD8+ T cell pool with predictive potential in non-small-cell lung cancer treated with PD-1 blockade. *Nat Med* 2018;24:994–1004.

21 Bronte V, Brandau S, Chen S-H, *et al*. Recommendations for myeloid-derived suppressor cell Nomenclature and characterization standards. *Nat Commun* 2016;7:12150.

22 Havel JJ, Chowell D, Chan TA. The evolving landscape of biomarkers for checkpoint inhibitor immunotherapy. *Nat Rev Cancer* 2019;19:133–50.

23 Manjarrez-Orduño N, Menard LC, Kansal S, *et al*. Circulating T cell subpopulations correlate with immune responses at the tumor site and clinical response to PD1 inhibition in non-small cell lung cancer. *Front Immunol* 2018;9:1613.

24 Tietze JK, Angelova D, Heppt MV, *et al*. The proportion of circulating CD45RO+CD8+ memory T cells is correlated with clinical response in melanoma patients treated with ipilimumab. *Eur J Cancer* 2017;75:268–79.

25 Kunert A, Basak EA, Hurkmans DP, *et al*. CD45RA+CCR7- CD8 T cells lacking co-stimulatory receptors demonstrate enhanced frequency in peripheral blood of NSCLC patients responding to nivolumab. *J Immunother Cancer* 2019;7:149.

26 Sathaliyawala T, Kubota M, Yudanin N, *et al*. Distribution and compartmentalization of human circulating and tissue-resident memory T cell subsets. *Immunity* 2013;38:187–97.

27 Joshi NS, Cui W, Chandele A, *et al*. Inflammation directs memory precursor and short-lived effector CD8(+) T cell fates via the graded expression of T-bet transcription factor. *Immunity* 2007;27:281–95.

28 Herndler-Brandstetter D, Ishigame H, Shinnakasu R, *et al*. KLRG1+ Effector CD8+ T Cells Lose KLRG1, Differentiate into All Memory T Cell Lineages, and Convey Enhanced Protective Immunity. *Immunity* 2018;48:716–29.

29 Wei SC, Levine JH, Cogdill AP, *et al*. Distinct cellular mechanisms underlie anti-CTLA-4 and anti-PD-1 checkpoint blockade. *Cell* 2017;170:1120–33.

30 Liakou CI, Kamat A, Tang DN, *et al*. CTLA-4 blockade increases IFNgamma-producing CD4+ICOShi cells to shift the ratio of effector to regulatory T cells in cancer patients. *Proc Natl Acad Sci U S A* 2008;105:14987–92.

31 Ng Tang D, Shen Y, Sun J, *et al*. Increased frequency of ICOS+ CD4 T cells as a pharmacodynamic biomarker for anti-CTLA-4 therapy. *Cancer Immunol Res* 2013;1:229–34.

32 Kamphorst AO, Pillai RN, Yang S, *et al*. Proliferation of PD-1+ CD8 T cells in peripheral blood after PD-1-targeted therapy in lung cancer patients. *Proc Natl Acad Sci U S A* 2017;114:4993–8.

33 Huang AC, Orlowski RJ, Xu X, *et al*. A single dose of neoadjuvant PD-1 blockade predicts clinical outcomes in resectable melanoma. *Nat Med* 2019;25:454–61.

34 Williford J-M, Ishihara J, Ishihara A, *et al*. Recruitment of CD103+ dendritic cells via tumor-targeted chemokine delivery enhances efficacy of checkpoint inhibitor immunotherapy. *Sci Adv* 2019;5:eaay1357.

35 Molgora M, Esaulova E, Vermi W, *et al*. Trem2 modulation remodels the tumor myeloid landscape enhancing anti-PD-1 immunotherapy. *Cell* 2020;182:886–900.

36 Bergenfelz C, Larsson A-M, von Stedingk K, *et al*. Systemic monocytic-MDSCs are generated from monocytes and correlate with disease progression in breast cancer patients. *PLoS One* 2015;10:e0127028.

37 Wang Q, Guldner IH, Golomb SM, *et al*. Single-cell profiling guided combinatorial immunotherapy for fast-evolving CDK4/6 inhibitor-resistant HER2-positive breast cancer. *Nat Commun* 2019;10:1–12.

38 Xue J, Schmidt SV, Sander J, *et al*. Transcriptome-Based network analysis reveals a spectrum model of human macrophage activation. *Immunity* 2014;40:274–88.

39 Murray PJ. Macrophage polarization. *Annu Rev Physiol* 2017;79:541–66.

40 Cassetta L, Fragkogianni S, Sims AH, *et al*. Human tumor-associated macrophage and monocyte transcriptional landscapes reveal cancer-specific reprogramming, biomarkers, and therapeutic targets. *Cancer Cell* 2019;35:588–602.

41 Kitamura T, Doughty-Shenton D, Cassetta L, *et al*. Monocytes differentiate to immune suppressive precursors of metastasis-associated macrophages in mouse models of metastatic breast cancer. *Front Immunol* 2017;8:2004.

42 Spranger S, Dai D, Horton B, *et al*. Tumor-Residing Batf3 dendritic cells are required for effector T cell trafficking and adoptive T cell therapy. *Cancer Cell* 2017;31:711–23.

43 Garris CS, Arlauckas SP, Kohler RH, *et al*. Successful anti-PD-1 cancer immunotherapy requires T Cell-Dendritic cell crosstalk involving the cytokines IFN-γ and IL-12. *Immunity* 2018;49:1148–61.

44 SA O, D-C W, Cheung J. PD-L1 expression by dendritic cells is a key regulator of T-cell immunity in cancer. *Nat Cancer* 2020;1:681–91.